

Surface-directed spinodal decomposition: Phenomenology and numerical results

Sanjay Puri* and Kurt Binder

Institut für Physik, Johannes Gutenberg Universität Mainz, D 6500 Mainz, Staudinger Weg 7, Germany
(Received 17 June 1991; revised manuscript received 4 May 1992)

We present a phenomenological theory for surface effects on spinodal decomposition in mixtures and related phenomena such as the dynamics of surface segregation. Numerical solutions of our equations show striking similarity to recent results from experiments on polymer mixtures with one component preferentially attracted to a wall.

PACS number(s): 68.10.-m, 05.70.Fh, 64.75.+g

There has been considerable interest in the dynamics of segregation (e.g., spinodal decomposition) of binary mixtures quenched below their critical temperature T_c [1]. Experiments and numerical simulations have now conclusively demonstrated that, in the absence of hydrodynamic effects, the segregation process is characterized by a unique, time-dependent length scale $l(t)$ (where t is time), which behaves asymptotically as $l(t) \sim t^{1/3}$. Until recently, the growth exponent (and even the existence of a power-law behavior) has been the subject of some controversy and much attention has focused on extracting this exponent numerically. As a consequence, scant attention has been paid to more intricate and physically important problems, e.g., the effect of surfaces on systems which undergo segregation [2,3]. Typically, given a binary mixture AB , it is possible that one of the components may be preferentially attracted to or repelled from a surface. This preference of the surface for a particular component is expected to produce strong effects near the surface at tem-

peratures both above and below T_c , the critical temperature in the bulk. A recent experiment [4] has shown the existence of surface-directed spinodal decomposition waves in binary polymer mixtures when one of the polymers is preferentially attracted to the surface. In this paper, we present a numerical study (based on a phenomenological theory) of the rather dramatic effects which are introduced by the presence of a surface.

The starting point for our numerical study is a variant on a model proposed recently by Binder and Frisch [5]. Starting off from a semi-infinite Ising model with Kawasaki spin exchange dynamics, Binder and Frisch [5] apply the master equation approach [6] to derive the Cahn-Hilliard (CH) equation in the bulk [7] with two special boundary conditions which model the presence of the surface. For the case of a system that is homogeneous in directions parallel to the surface (assumed to lie on the plane $z=0$), their bulk equation is the usual CH equation,

$$2\tau_s \frac{\partial \psi(z,t)}{\partial t} = - \frac{\partial^2}{\partial z^2} \left[\left(\frac{T_c}{T} - 1 \right) \psi(z,t) - \frac{1}{3} \psi(z,t)^3 + \frac{J}{T} \frac{\partial^2 \psi(z,t)}{\partial z^2} \right] \quad (z > 0), \quad (1)$$

where $\psi(z,t)$ is the order parameter at the point z at time t [$\psi(z,t) \sim \rho_A(z,t) - \rho_B(z,t)$, where $\rho_A(z,t)$ and $\rho_B(z,t)$ are respectively the densities of the species A and B]. In (1), τ_s is the time scale that characterizes the underlying microscopic dynamics; T is the temperature; and $T_c (=qJ$, where q is the coordination number and J is the bulk exchange interaction of the underlying microscopic model) is the bulk critical temperature. The first boundary condition is

$$2\tau_s \frac{\partial \psi(0,t)}{\partial t} = \frac{H}{T} + \frac{J}{T} \left[(q-2) \frac{J_s}{J} - (q-1) \right] \psi(0,t) - \left[\frac{T_c}{T} - 1 - \frac{J}{T} \right] \frac{\partial \psi(z,t)}{\partial z} \Big|_{z=0} - \frac{1}{2} \left[\frac{T_c}{T} - 1 + \frac{J}{T} \right] \frac{\partial^2 \psi(z,t)}{\partial z^2} \Big|_{z=0} - \frac{1}{6} \left[\frac{T_c}{T} - 1 + \frac{5J}{T} \right] \frac{\partial^3 \psi(z,t)}{\partial z^3} \Big|_{z=0}, \quad (2)$$

where the parameter J_s is the exchange interaction between sites on the surface in the underlying microscopic model and H is a field on the surface which models the preference of the surface for one of the components. This boundary condition describes the dynamics of the order parameter on the surface as a result of the surface field and the one-sided gradients due to the absence of material in the $-z$ direction. It has the physical effect of rapidly pinning the order-parameter value on the surface to the value dictated by static requirements. For the second boundary condition, we use (differing from Binder and Frisch [5]) the manifestly order-parameter-conserving condition

$$\frac{\partial}{\partial z} \left[\left(\frac{T_c}{T} - 1 \right) \psi(z,t) - \frac{1}{3} \psi(z,t)^3 + \frac{J}{T} \frac{\partial^2 \psi(z,t)}{\partial z^2} \right] \Big|_{z=0} = 0. \quad (3)$$

By an appropriate rescaling of $\psi(z,t)$, z , and t [8], we can set (1)–(3) in the dimensionless form

$$\frac{\partial \phi(x, \tau)}{\partial \tau} = -\frac{\partial^2}{\partial x^2} \left[\text{sgn}(T_c - T) \phi(x, \tau) - \phi(x, \tau)^3 + \frac{1}{2} \frac{\partial^2 \phi(x, \tau)}{\partial x^2} \right] \quad (x > 0), \quad (4)$$

with the boundary conditions

$$\frac{\partial \phi(0, \tau)}{\partial \tau} = h + g\phi(0, \tau) + \gamma \frac{\partial \phi(x, \tau)}{\partial x} \Big|_{x=0} - \left(\frac{\gamma}{4} \right)^{2/3} \frac{\partial^2 \phi(x, \tau)}{\partial x^2} \Big|_{x=0} - \frac{5}{6} \left(\frac{\gamma}{4} \right)^{1/3} \frac{\partial^3 \phi(x, \tau)}{\partial x^3} \Big|_{x=0} \quad (5)$$

and

$$\frac{\partial}{\partial x} \left[\phi(x, \tau) - \phi(x, \tau)^3 + \frac{1}{2} \frac{\partial^2 \phi(x, \tau)}{\partial x^2} \right] \Big|_{x=0} = 0, \quad (6)$$

where $\phi(x, \tau)$ is the scaled order parameter as a function of scaled distance x and time τ . The scaled parameters in (4)–(6) are

$$\begin{aligned} h &= \frac{4H}{\sqrt{3}T} \left(\frac{T}{T_c} \right)^{3/2} (2q)^{3/2} \xi^5, \\ g &= 8 \left[(q-2) \frac{J_s}{J} - (q-1) \right] \xi^4, \\ \gamma &= 4\xi^3, \end{aligned} \quad (7)$$

where $\xi [= (2q|1 - T/T_c|)^{-1/2}]$ is the bulk correlation length. Strictly speaking, the approximations that lead to (1)–(3) and (4)–(6) are only justifiable close to the critical temperature. Nevertheless, given our experience with similar problems, we consider these equations as providing a reasonable phenomenological description over the entire temperature range. Furthermore, we remark that the static description derived from (4)–(6) (by putting $\partial/\partial\tau \equiv 0$) matches (as it should) the static description for the case with nonconserved order parameter [9]. Thus, we can invoke the phase diagram of Ref. [9] to recognize the static equilibria (i.e., whether wet or nonwet) to which various choices of parameters in our model correspond. Of course, the situation here is complicated by the constraint that the order parameter be conserved so that our simulations only see local wetting at the surfaces as opposed to global wetting in the nonconserved case [9].

We have studied (4)–(6) numerically for temperatures T both above and below T_c . For simplicity, we do not address here the more delicate question of what happens precisely at the critical temperature (where thermal fluctuations are relevant). All results presented here are for critical mixtures with equal concentrations of the components A and B .

For temperatures below T_c , the bulk tends to spontaneously segregate into its constituent components (spinodal decomposition). Figure 1(a) shows the order parameter profiles (near the surface) obtained from a numerical integration of (4)–(6) on a line of length $L=60$ with mesh sizes $\Delta\tau=0.001$ and $\Delta x=0.4$. The parameter values were $h=4$, $g=-4$, and $\gamma=4$, which correspond to a nonwet static equilibrium [9]. These profiles are obtained by averaging over 80 runs from independent initial conditions, each consisting of uniformly distributed random fluctuations of amplitude 0.05 about a zero background. In the bulk [not shown in Fig. 1(a)], the composition

waves have randomly oriented wave vectors and random phases and the averaging gives a bulk value of $\phi(x, \tau)$, which is approximately zero. However, things are different near the surface [shown in Fig. 1(a)], which has a preference for the component A (in our terminology). Near the surface, one sees spinodal decomposition waves with a wave vector normal to the surface. These waves propagate in from the surface. These numerical results duplicate the experimental profiles of Jones *et al.* [4], who report similar spinodal decomposition waves in a polymer mixture, with one of the polymers having a preferential attraction to the surface. These spinodal decomposition waves are characterized by (typically) the distance of the first zero crossing [$R_1(\tau)$] or second zero crossing [$R_2(\tau)$] from the surface. In Fig. 1(b), we plot $R_1(\tau)$

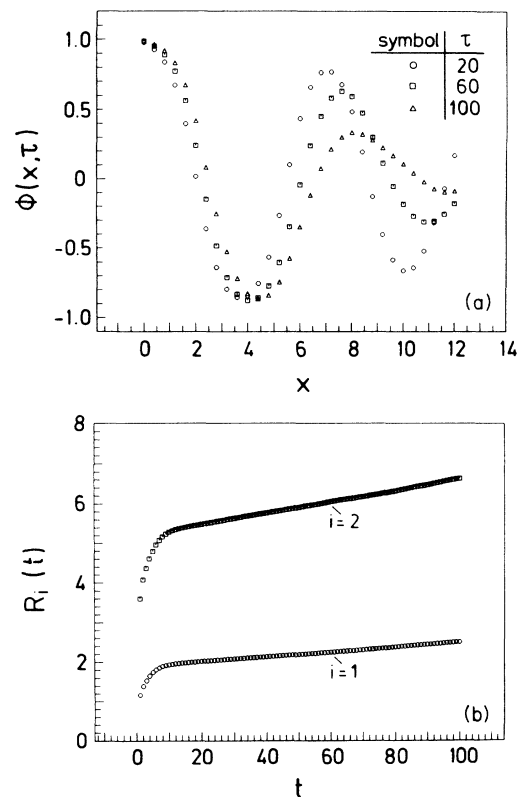


FIG. 1. (a) Surface-directed spinodal decomposition waves at dimensionless times 20, 60, and 100 (denoted by the symbols indicated) obtained from a numerical simulation of (4)–(6), as described in the text. The parameter values are $h=4$, $g=-4$, and $\gamma=4$. The profiles rapidly decay to zero in the bulk, which is not shown here. (b) Temporally linear growth of $R_1(\tau)$ and $R_2(\tau)$, the first and second zero crossing of the spinodal decomposition waves of (a).

and $R_2(\tau)$ vs τ . After an initial transient regime, both $R_1(\tau)$ and $R_2(\tau)$ increase linearly in time but with slightly different velocities. These provide a measure of the growth of the enrichment domain (A -rich) at the surface and the depletion domain (B -rich) adjacent to it.

It is also interesting to note that a degree of surface enrichment can occur for $T > T_c$ if an appropriate field is applied at the surface. Figure 2 shows the enrichment profiles for an initially homogeneous state ($\phi = 0$) with a surface field $h = 4$ turned on at time $\tau = 0$. The mesh sizes and parameters in this simulation are the same as those for Fig. 1. Figure 2 shows that the surface rapidly becomes rich in the A component. Because of the conservation constraint, the system becomes rich in the other component B beyond a time-dependent length scale $R_1(\tau)$ and the profile decays off to 0 in the bulk. We have confirmed that the time-dependent profile is well fitted by the double exponential

$$\phi(x, \tau) = B_-(\tau)e^{-x/\xi_-(\tau)} - B_+(\tau)e^{-x/\xi_+(\tau)}, \quad (8)$$

where $B_-(\tau), B_+(\tau) > 0$. The functions $B_-(\tau)$ and $\xi_-(\tau)$ rapidly saturate out to their static equilibrium values whereas $B_+(\tau) \sim \tau^{-1/2}$ and $\xi_+(\tau) \sim \tau^{1/2}$. It is interesting to note that the various moments of the profile show a power-law behavior in time as $\langle x^n \rangle \sim \tau^{n/2}$ but the first zero of the profile behaves as $R_1(\tau) \sim \ln \tau$. This is reminiscent of the logarithmic growth of the wetting layer in the case with nonconserved order parameter [9].

To summarize, starting from a nonlinear diffusion equation with suitable boundary conditions, we have been able to describe the anisotropy that walls induce in structures forming via phase separation. Consistent with recent experiments on polymer mixtures [4], we have found that the surface acts like a pinning center for the maximum amplitude of a growing concentration wave, with wave vector perpendicular to the wall. We feel that such

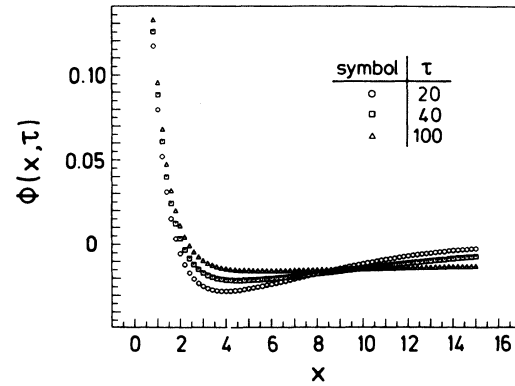


FIG. 2. Enrichment profiles for dimensionless times 20, 40, and 100 (denoted by the symbols indicated) for $T > T_c$. Surface enrichment is the result of a field $h = 4$ applied at the surface, other parameters being $g = -4$ and $\gamma = 4$. The profiles are well approximated by the double exponential form described in the text.

phenomena should have widespread and important consequences for the physical properties of surfaces of materials. The effects described here should be particularly relevant for the recently advancing technology of layered materials with suitably "tailored" microstructures, recalling that intermediate stages of phase separation can be frozen in by quenching the system to very low temperatures where the atomic mobility is small.

S.P. is grateful to the Deutsche Forschungsgemeinschaft (DFG) for supporting his stay at Mainz under Sonderforschungsbereich 262. K.B. is grateful to R. A. L. Jones and E. J. Kramer for informing him of Ref. [4] prior to its publication.

*Permanent address: School of Physical Sciences, Jawaharlal Nehru University, New Delhi, 10067, India.

- [1] For reviews, see J. D. Gunton, M. San Miguel, and P. S. Sahni, in *Phase Transitions and Critical Phenomena*, edited by C. Domb and J. L. Lebowitz (Academic, New York, 1983), Vol. 8, p. 267.
- [2] J. Rowlinson and B. Widom, *Molecular Theory of Capillarity* (Oxford Univ. Press, Oxford, 1982).
- [3] K. Binder, in *Phase Transitions and Critical Phenomena* (Ref. [1]), p. 1; P. G. de Gennes, *Rev. Mod. Phys.* **57**, 827

(1985).

- [4] R. A. L. Jones, L. J. Norton, E. J. Kramer, F. S. Bates, and P. Wiltzius, *Phys. Rev. Lett.* **66**, 1326 (1991).
- [5] K. Binder and H. L. Frisch, *Z. Phys. B* **84**, 403 (1991).
- [6] K. Binder, *Z. Phys.* **267**, 313 (1974).
- [7] J. W. Cahn and J. E. Hilliard, *J. Chem. Phys.* **28**, 258 (1958); **31**, 688 (1959).
- [8] S. Puri and K. Binder (unpublished).
- [9] I. Schmidt and K. Binder, *Z. Phys. B* **67**, 369 (1987); S. Puri and K. Binder, *ibid.* **86**, 263 (1992).